Atmos. Meas. Tech. Discuss., 8, 5265–5282, 2015
www.atmos-meas-tech-discuss.net/8/5265/2015/
doi:10.5194/amtd-8-5265-2015
© Author(s) 2015. CC Attribution 3.0 License.

Atmospheric Measurement Techniques Discussions

This discussion paper is/has been under review for the journal Atmospheric Measurement Techniques (AMT). Please refer to the corresponding final paper in AMT if available.

Probing ice-nucleation processes on the molecular level using second harmonic generation spectroscopy

A. Abdelmonem[1], **J. Lützenkirchen**[2], **and T. Leisner**[1]

[1]Institute of Meteorology and Climate Research – Atmospheric Aerosol Research (IMKAAF), Karlsruhe Institute of Technology (KIT), 76344 Eggenstein-Leopoldshafen, Germany
[2]Institute of Nuclear Waste Disposal (INE), Karlsruhe Institute of Technology (KIT), 76344 Eggenstein-Leopoldshafen, Germany

Received: 23 February 2015 – Accepted: 30 April 2015 – Published: 22 May 2015

Correspondence to: A. Abdelmonem (ahmed.abdelmonem@kit.edu)

Published by Copernicus Publications on behalf of the European Geosciences Union.

Abstract

We present and characterize a novel setup to apply Second Harmonic Generation (SHG) spectroscopy in total internal reflection geometry (TIR) to heterogeneous freezing research. It allows to monitor the evolution of water structuring at solid surfaces at low temperatures prior to heterogeneous ice nucleation. Apart from the possibility of investigating temperature dependence, a major novelty in our setup is the ability of measuring sheet-like samples in TIR geometry in a direct way. As a main experimental result, we find that our method can discriminate between good and poor ice nucleating surfaces. While at the sapphire basal plane, which is known to be a poor ice nucleator, no structural rearrangement of the water molecules is found prior to freezing, the basal plane surface of mica, an analogue to ice active mineral dust surfaces, exhibits a strong change in the nonlinear optical properties at temperatures well above the freezing transition. This is interpreted as a pre-activation, i.e. an increase in the local ordering of the interfacial water which is expected to facilitate the crystallization of ice at the surface. The results are in line with recent predictions by Molecular Dynamics simulations on a similar system.

1 Introduction

Immersion freezing, i.e. the formation of ice on the surface of an insoluble aerosol particle (the ice nucleating particle, INP) in a supercooled droplet of water or an aqueous solution is the most important mode for formation of atmospheric ice (Pruppacher and Klett, 1997). It facilitates the initiation of precipitation and is largely responsible for the formation of cirrus clouds, which modify the global energy budget (Zhang et al., 1999). Despite its importance, little is known about the molecular structure of the critical ice nucleus and how it is stabilized by the interaction with aerosol surfaces.

Atmospheric aerosols can enhance heterogeneous Ice Nucleation (IN) in the deposition, contact and immersion mode. In the latter case, an insoluble aerosol particle

AMTD
8, 5265–5282, 2015

immersed within a droplet of supercooled water or aqueous solution eventually leads to the formation of ice well above the temperature of homogeneous freezing (Pruppacher and Klett, 1997). Immersion freezing on mineral dust particles or primary biological particles is the dominant mode of heterogeneous freezing in the atmosphere (Korolev and Isaac, 2003; Pruppacher and Klett, 1997). Experimental immersion freezing studies of heterogeneous IN show a wide variability in behaviour among the different atmospheric particles that are considered relevant (see Hoose and Mohler, 2012 and references therein).

It remains elusive which physical, structural and chemical characteristics of the INPs account for this variability and which aspects are dominant (Anim-Danso et al., 2013a; Conrad et al., 2005; Hu and Michaelides, 2007). Recent Molecular Dynamic (MD) simulations on heterogeneous IN of water on carbon surfaces suggest that good ice nucleators induce layering of liquid water at the surface (Lupi et al., 2014; Lupi and Molinero, 2014). Those authors proposed that such layering of water enhances the local ordering of the first water layer in contact with the surface. So far, no classification of ice nucleation abilities based on the chemical or physical properties of a potential ice nucleator has been published and hardly any laboratory based information is available neither on the molecular structure of the surface active sites and its role in the IN process nor on the molecular structure of the critical germ of water. Various methods have been employed to study heterogeneous IN, e.g. infra-red spectroscopy (Richardson et al., 2007; Sadtchenko and Ewing, 2011). Following this, one promising approach to elucidate these structures on the molecular level is nonlinear optical (NLO) spectroscopy. Second Harmonic Generation (SHG) and Sum Frequency Generation (SFG) are powerful surface sensitive spectroscopic tools for studying molecules near surfaces and at interfaces (Shen, 1989). The amplitude and polarization of the generated field, as a function of the polarization of the incident fields, carries information on the orientation of the interfacial molecules (Abdelmonem, 2008; Jang et al., 2013; Rao et al., 2003; Zhuang et al., 1999).

AMTD
8, 5265–5282, 2015

The structure of water molecules adsorbed on a mica surface has been previously studied at room temperature using SFG spectroscopy (Miranda et al., 1998). More recently Yang et al. employed SFG spectroscopy at the liquid water/mica interface to explore the role of sulfuric acid coatings on mineral dust particles in IN (Yang et al., 2011). They found that the signal emerging from ordered water structures on the mica surface decreased above a concentration of 0.5 M of H_2SO_4 and disappeared above 5 M of H_2SO_4. This was taken as indirect evidence that ordering of water at the INP is related to ice nucleation. A very recent study on IN processes using SFG focused on the structure of ice as well as freezing and melting transition temperatures for water in contact with the sapphire-c (basal) plane (Anim-Danso et al., 2013a). Those authors compared the amplitude of "ice-like" and "water-like" peaks in the SFG spectra at different pH values just before and immediately after the freezing transition, but did not follow the evolution of the SFG signal when approaching the freezing transition. One major focus was the influence of the surface charge in enhancing or delaying ice formation. Subsequent studies from the same group addressed the role of salt hydrates during freezing (Anim-Danso et al., 2013b; Zhang et al., 2014). So far no comparison between different surfaces has been published in order to evaluate their concomitant ability as ice nucleator.

In this work we demonstrate a novel setup which uses SHG, in total internal reflection (TIR) geometry, to probe water structuring at the interface upon supercooling. TIR measurements for a sheet-like sample (mica) is achieved by coupling the light from a prism-like sapphire single crystal using an appropriate index matching gel (IMG). The choice of the IMG material is explained in detail. An IN cell is integrated to the setup using a precise temperature-controlled (down to −195 °C) cold stage. Two mineral surfaces are used as atmospheric aerosol analogues. Sapphire (α-Al_2O_3) is considered to be a poor ice nucleator (Thomas, 2009; Richardson, 2006) while mica (a layered clay mineral: $KAl_2[AlSi_3O_{10}(OH)_2]$) is believed to be among the most effective ice nucleating minerals (Eastwood et al., 2008; Glaccum and Prospero, 1980). The evolution of water structuring, upon supercooling on the surface of mica is compared to that at the surface

AMTD
8, 5265–5282, 2015

of sapphire. A sapphire prism was used as a substrate in sapphire/water experiments and as an optical-coupler for mica substrates in the mica/water experiments. The focus of this article is to demonstrate the usefulness of the technique and to present first results on temperature dependent structural changes of water on the surfaces of sapphire and mica on cooling and discuss the findings in the light of the IN abilities of these surfaces. We are working far from any resonant second-order susceptibility $\chi_R^{(2)}$, and the $\chi_{NR}^{(3)}$ effect is ignored since we do not track ion adsorption at the interface (Ong et al., 1992).

2 Experimental

2.1 Materials and setup

All experiments are carried out using MilliQ water (18.2 M Ω cm). The total organic content in this water is below 4 ppb. The sapphire prisms are obtained from Victor Kyburz AG, Safnern, Switzerland. The roughness of the sapphire surface is 1.5 nm and the flatness is lambda/4. Mica Samples (Muscovite $KAl_2[AlSi_3O_{10}(OH)_2]$) are obtained from Plano GmbH, Germany. The mica samples are freshly cleaved in air. Both minerals used here expose their basal-planes and are probed in TIR geometry. The contact angles of the neat sapphire-c and mica surfaces with water are 30 and 0° respectively. The contact angle measurements were carried out both by the drop method and by the plate method for sapphire, while for mica, only the drop method was used. Changes in the amount of dissolved gases are assumed to be minimal since the cell is closed. Furthermore, a possible effect of dissolved gas on the ice-nucleation behavior would be the same for both surfaces so that this is unlikely to affect the outcome.

For our experiments, we use a two-beam-SHG setup in TIR geometry (cf. Fig. 1). A sapphire prism is used either directly as a substrate exposing the surface of interest or as an optical coupler to the surface of thin mica substrates. Both substrates ultimately expose their basal-planes to liquid water or water vapor. To be able to study

AMTD
8, 5265–5282, 2015

mica, an index matching gel (IMG) is used to fix the mica sample on the hypotenuse of the sapphire prism (see details below).

As a further novelty, the setup is integrated into a temperature controlled environmental chamber to study temperature dependent signals. We used a commercially available cold-stage (Linkam model HFS-X350) and modified the housing to accommodate the SHG setup. Control software is developed to perform a predefined temperature profile and to collect the SHG signal, the reflectivities of the incident beams, and the temperature of the sapphire prism at two positions surrounding the point of laser interaction and of the fluid phase above the interface. Temperature profiles are repeated several times for each sample to test reproducibility. First they were applied to sapphire/N_2 and mica/N_2 (i.e. solid/gas) interfaces to assure that the change in the refractive indices of the substrates and IMG with temperature has no significant effect on the resulting SHG signal in the range of temperatures applied in this work. The SHG experiments are conducted using a femtosecond laser system (Solstice, Spectra Physics) with a fundamental beam of 800 nm wavelength, 3.5 mJ pulse energy, ~ 80 fs pulse width, 1 kHz repetition rate, and a beam diameter of 1 mm at the interface. Only 30 % of the laser output power is coupled to the setup. The TIR geometry provides an additional enhancement of the SHG signal if the incident beams are close to the critical angle (Abdelmonem, 2008). Instead of having a single fundamental beam incident on the interface, two incident beams at two different angles are allowed to overlap in space and time at the interface similar to SFG setups. This allows better separation between the background accompanying the fundamental beam and the signal from the probed interface (cf. Fig. 1). The fundamental beam is split in two paths (B1 and B2) using a 50 % beam splitter. The two split wave fronts of each pulse are spatially and temporally overlapped at the interface. Equal optical paths on both arms are achieved via a delay unit placed in the path of B1. The polarization direction of the incident beams is controlled by a half-wave plate followed by a cube polarizer. The generated signal is collected using a photomultiplier tube (PMT) placed beyond an optical system, which includes appropriate filters and a polarization analyzer. The experiments are carried

AMTD
8, 5265–5282, 2015

out using two incident beams where B1 is adjusted to be at an angle slightly above the critical angle to avoid changes in signal due to the strong temperature dependence of the Fresnel coefficients at the critical angle. A fast video camera (Guppy F-036, Allied Vision Technology) is used to image macroscopic layers of water or ice on the crystal surface.

The SHG response is sensitive to the overall arrangements of the dipole moments of the interfacial water molecules (Fordyce et al., 2001; Goh et al., 1988; Luca et al., 1995). Two polarization combinations are required to describe the water system which has C_{2v} symmetry. We denote by P or S a polarization parallel or perpendicular to the plane of incidence, respectively. PPP polarization combination corresponds to P-SHG, P-B2 and P-B1 and SSP polarization combination corresponds to S-SHG, S-B2 and P-B1. The stronger the signal of either SSP or PPP, the more pronounced is the ordering of the molecules, while the ratio of SSP/PPP determines the average orientation of the interfacial (water) molecules (Abdelmonem, 2008). In this work we use PPP only to qualitatively follow the structural change of water molecules.

The substrate of interest is sealed to a circular opening of diameter 8 mm in a Teflon cell which can be filled with water or humid air. One of the two prism sides perpendicular to the hypotenuse is mounted on the cold stage. The temperatures of sample top, sample bottom and water (or air) inside the cell are recorded using four-wire-Pt100 elements. However, we are not interested here in the exact onset conditions of freezing, but rather study the qualitative behavior of water molecules during supercooling.

It is impossible to achieve the desired TIR geometry using substrates that are only available as plate-like samples as mica. Mica has a refractive index ($n_m = 1.564$) lower than that of sapphire ($n_s = 1.7522$) and higher than that of water ($n_w = 1.329$), at 800 nm. This allows access to the mica/water interface using the TIR geometry by applying an IMG between sapphire and mica, see inset Fig. 1. An IMG ($n_g = 1.45186$) from Thorlabs is used in the present case. It satisfies the condition that there is no TIR at the sapphire/IMG or IMG/mica interface but at the mica/water interface. With our

AMTD
8, 5265–5282, 2015

sample geometry, the appropriate incident angle of light from air (θ_a) ranges from ~ 7.1 to ~ 18.9° (see Sect. 2.2 for details).

2.2 Selection of optimum IMG

For better beam coupling (i.e. larger acceptance angle), the refractive index of the IMG can be optimized to simultaneously maximize the critical angle of TIR at both sapphire/IMG and IMG/mica interfaces. We find that the optimum value for our system is $n_g \geq n_m$. The reflectivities at the sapphire/IMG, IMG/mica and mica/water interfaces of a P-polarized light as a function of the incident angle from air (θ_a) are plotted in Fig. 2. A similar treatment is possible for S-polarized light. An arbitrary value ($n_g = 1.575$) is used for the illustrative calculations shown on this plot. The suitable range of θ_a should have a minimum higher than those corresponding to the critical angles of TIR at sapphire/IMG and IMG/mica interfaces (the points of drop of the solid-red and dashed-green curves) and a maximum lower than that for mica/water interface (the point of drop of the long-dashed-blue curve). At lower angles the beam is totally reflected at the sapphire/IMG or IMG/mica interface and at higher angles the beam violates the TIR condition at the mica/water interface. The inset in Fig. 2 shows the points of drop of the reflectivity for the three interfaces (lower and higher thresholds of θ_a) as a function of n_g. The shaded area is the range of suitable incident angles from air at any n_g. In our study we used an IMG with $n_g = 1.45186$. The corresponding appropriate incident angle of light from air (θ_a) ranges from ~ 7.1 to ~ 18.9°.

3 Results and discussion

We explore immersion freezing, i.e. water molecule ordering and ice formation at the interface between the crystal and bulk water. For this purpose, the cell was filled with pure water and a cooling ramp is applied to the whole system. Figure 3a shows the change in the SHG signal at the sapphire/water interface for a cooling profile from 10

AMTD
8, 5265–5282, 2015

to about −15 °C. The cooling profile (cooling rate: 8 °C min^{-1}) is repeated five times to confirm the reproducibility of the result. The SHG signal shows a slight decrease with temperature before the phase change. A step is observed at the phase transition (ice/sapphire interface). Other cooling profiles with different cooling rates (17, 14, 11, 8, 4 and 2 °C min^{-1}) in the same temperature range did not lead to different results (see Fig. 3b). The slight change in the SHG before the phase change could be due to temperature dependence of the optical properties of water and sapphire. Similar observations were reported for the range between 20 and 70 °C (Zhang et al., 2005). The slight temperature increase after the phase change is due to the release of latent heat.

In contrast, Fig. 4 shows the evolution of the SHG signal generated at the mica/water interface for a cooling profile in the same range of that of sapphire/water interface. The cooling profile is repeated 4 times at the same rate (2 °C min^{-1}). Well before the phase transition, the SHG signal is rising. This observation suggests an enhancement in the local ordering of the interfacial water in contact with the surface upon supercooling (a pre-activation). This process in turn is expected to facilitate ice crystallization at the surface. Water molecules form strong hydrogen bonds with their neighbours upon cooling and gradually start to fit into positions that resemble the hexagonal packing achieved upon freezing (Smith, 2004). Here, we find indications that this hexagonal packing is probably facilitated by the mica-surface since it induces pre-packing in the liquid phase. Recently it was reported that freezing at air/water interfaces does not proceed via the hexagonal basal face (Shultz et al., 2014). Even though the mica samples were freshly cleaved before each experiment small variations were observed at high temperatures (see Fig. 4), but the trend was always the same and different from that observed consistently with sapphire. While it is the focus of this paper to demonstrate the ability of this technique to observe variations at the interface of different aerosol surfaces, we plan to investigate the origin of the observed mica behavior in a separate study. Figure 4 shows the typically observed relation.

AMTD
8, 5265–5282, 2015

From the present results we cannot know the precise position at which the ice nucleation starts. Once the critical germ forms at any point, freezing propagates along the surface at a rate of about 0.1 $m\,s^{-1}$ (Rauschenberger et al., 2013; Shibkov et al., 2003, 2005). The video recording could determine that the ice phase was nucleated at the interface between the crystal surface and the cell opening and subsequently propagated through our optically probed region. However, experimentally we show that the technique is able to resolve a pre-activation induced by the surface of a good ice nucleator. Our results agree with the theoretical predictions by Lupi et al. (2014) which show that good ice nucleators induce layering of the liquid water which in turn enhances the local ordering of the first water layer in contact with the surface (Lupi et al., 2014; Lupi and Molinero, 2014).

4 Conclusions

We have demonstrated the capability of a novel system to investigate heterogeneous ice nucleation on the molecular level before, during and after the phase change. Sheet-like sample could be studied in TIR geometry by applying a suitable IMG between the sample and a prism-like optical coupler. The selection of an appropriate IMG for such purposes is discussed. Immersion freezing was studied on surfaces of two different minerals that are known to be poor and good ice nucleators, respectively. Sapphire, as a model surface of a poor IN agent, showed no influence on the water structure at its surface upon cooling down to the point of freezing. However, mica, as a good IN agent, induced local ordering of the first water layer in contact with the surface which is represented by the enhancement of the SHG upon cooling. This strong ordering of water molecules is expected to facilitate the crystallization of ice at the surface. This fits well to the recent theoretical findings on graphite (Lupi et al., 2014). To our knowledge, this is the first experimental confirmation that heterogeneous ice crystallization on a surface is related to the degree of order induced by this surface to supercooled water. For more specific characterization of ice nucleation at mica/water interfaces and sim-

AMTD
8, 5265–5282, 2015

ilar systems, our setup should be enhanced to allow SFG studies to gain more direct orientational and dynamic information on the interfacial water molecules by tracking different specific vibrational bands, such as those of "liquid-like" and "ice-like" contributions. This will allow probing the structuring of water molecules and correlating ice nucleation efficiency to the structural and chemical characteristics of the surface. Further experiments on mica/water interface are essential to understand its behaviour in bare aquatic solutions.

Acknowledgements. The fund for building the SHG setup including the temperature controlled cold stage was received from the competence area "Earth and Environment" – KIT through a start-up budget (2012). The work was initiated with a start-up fund from the KIT and is currently funded by the German Research Foundation (DFG, AB 604/1-1).

The article processing charges for this open-access publication were covered by a Research Centre of the Helmholtz Association.

References

Abdelmonem, A.: Nonlinear optical spectroscopy at the Liquid-/Solid- interface, 1.0, Naturwissenschaften, Mathematik und Informatik, Ruprecht-Karls-Universität, Heidelberg, 2008.

Anim-Danso, E., Zhang, Y., Alizadeh, A., and Dhinojwala, A.: Freezing of water next to solid surfaces probed by infrared-visible sum frequency generation spectroscopy, J. Am. Chem. Soc., 135, 2734–2740, 2013a.

Anim-Danso, E., Zhang, Y., and Dhinojwala, A.: Freezing and melting of salt hydrates next to solid surfaces probed by infrared – visible sum frequency generation spectroscopy, J. Am. Chem. Soc., 135, 8496–8499, doi:10.1021/ja403437c, 2013b.

Conrad, P., Ewing, G. E., Karlinsey, R. L., and Sadtchenko, V.: Ice nucleation on BaF_2(111), J. Chem. Phys., 122, 064709–064711, doi:10.1063/1.1844393, 2005.

Eastwood, M. L., Cremel, S., Gehrke, C., Girard, E., and Bertram, A. K.: Ice nucleation on mineral dust particles: onset conditions, nucleation rates and contact angles, J. Geophys. Res.-Atmos., 113, 203–209, doi:10.1029/2008jd010639, 2008.

AMTD
8, 5265–5282, 2015

Fordyce, A. J., Bullock, W. J., Timson, A. J., Haslam, S., Spencer-Smith, R. D., Alexander, A., and Frey, J. G.: The temperature dependence of surface second-harmonic generation from the air-water interface, Mol. Phys., 99, 677–687, doi:10.1080/00268970010030022, 2001.
Glaccum, R. A. and Prospero, J. M.: Saharan aerosols over the tropical North Atlantic – Mineralogy, Mar. Geol., 37, 295–321, doi:10.1016/0025-3227(80)90107-3, 1980.
Goh, M. C., Hicks, J. M., Kemnitz, K., Pinto, G. R., Heinz, T. F., Eisenthal, K. B., and Bhattacharyya, K.: Absolute orientation of water molecules at the neat water surface, J. Phys. Chem., 92, 5074–5075, doi:10.1021/j100329a003, 1988.
Hoose, C. and Möhler, O.: Heterogeneous ice nucleation on atmospheric aerosols: a review of results from laboratory experiments, Atmos. Chem. Phys., 12, 9817–9854, doi:10.5194/acp-12-9817-2012, 2012.
Hu, X. L. and Michaelides, A.: Ice formation on kaolinite: lattice match or amphoterism?, Surf. Sci., 601, 5378–5381, doi:10.1016/j.susc.2007.09.012, 2007.
Jang, J. H., Lydiatt, F., Lindsay, R., and Baldelli, S.: Quantitative orientation analysis by sum frequency generation in the presence of near-resonant background signal: acetonitrile on rutile TiO_2 (110), J. Phys. Chem. A, 117, 6288–6302, doi:10.1021/jp401019p, 2013.
Korolev, A. and Isaac, G.: Phase transformation of mixed-phase clouds, Q. J. Roy. Meteor. Soc., 129, 19–38, doi:10.1256/qj.01.203, 2003.
Luca, A. A. T., Hebert, P., Brevet, P. F., and Girault, H. H.: Surface second-harmonic generation at air/solvent and solvent/solvent interfaces, J. Chem. Soc. Faraday T., 91, 1763–1768, doi:10.1039/ft9959101763, 1995.
Lupi, L. and Molinero, V.: Does hydrophilicity of carbon particles improve their ice nucleation ability?, J. Phys. Chem. A, 118, 7330–7337, doi:10.1021/jp4118375, 2014.
Lupi, L., Hudait, A., and Molinero, V.: Heterogeneous nucleation of ice on carbon surfaces, J. Am. Chem. Soc., 136, 3156–3164, doi:10.1021/ja411507a, 2014.
Miranda, P. B., Xu, L., Shen, Y. R., and Salmeron, M.: Icelike water monolayer adsorbed on Mica at room temperature, Phys. Rev. Lett., 81, 5876–5879, 1998.
Ong, S., Zhao, X., and Eisenthal, K. B.: Polarization of water molecules at a charged interface: second harmonic studies of the silica/water interface, Chem. Phys. Lett., 191, 327–335, doi:10.1016/0009-2614(92)85309-X, 1992.
Pruppacher, H. R. and Klett, J. D.: Microphysics of Clouds and Precipitation, 2nd rev., and enl. edn., Atmospheric and oceanographic sciences library, 18, Kluwer Academic Publishers, Dordrecht, Boston, 954 pp., 1997.

AMTD
8, 5265–5282, 2015

Rao, Y., Tao, Y.-S., and Wang, H.-F.: Quantitative analysis of orientational order in the molecular monolayer by surface second harmonic generation, J. Chem. Phys., 119, 5226–5236, doi:10.1063/1.1597195, 2003.
Rauschenberger, P., Criscione, A., Eisenschmidt, K., Kintea, D., Jakirlić, S., Tuković, Ž., Roisman, I. V., Weigand, B., and Tropea, C.: Comparative assessment of volume-of-fluid and level-set methods by relevance to dendritic ice growth in supercooled water, Comput. Fluids., 79, 44–52, doi:10.1016/j.compfluid.2013.03.010, 2013.
Richardson, H., Thomas, A., Carlson, M., Kordesch, M., and Govorov, A.: Thermo-optical responses of nanoparticles: melting of ice and nanocalorimetry approach, J. Electron. Mater., 36, 1587–1593, doi:10.1007/s11664-007-0279-1, 2007.
Richardson, H. H., Hickman, Z. N., Thomas, A. C., Dendramis, K. A., Thayer, G. E., and Ewing, G. E: Freezing of water on alpha-Al_2O_3 surfaces, The 11th International Conference on the Physics and Chemistry of Ice, Bremerhaven, Germany, 23–28 July 2006, p. 513, 2006.
Sadtchenko, V. and Ewing, G. E.: A new approach to the study of interfacial melting of ice: infrared spectroscopy, Can. J. Phys., 81, 333–341, doi:10.1139/p03-009, 2011.
Shen, Y. R.: Surface properties probed by second-harmonic and sum-frequency generation, Nature, 337, 519–525, 1989.
Shibkov, A. A., Golovin, Y. I., Zheltov, M. A., Korolev, A. A., and Leonov, A. A.: Morphology diagram of nonequilibrium patterns of ice crystals growing in supercooled water, Phys. A, 319, 65–79, doi:10.1016/S0378-4371(02)01517-0, 2003.
Shibkov, A. A., Zheltov, M. A., Korolev, A. A., Kazakov, A. A., and Leonov, A. A.: Crossover from diffusion-limited to kinetics-limited growth of ice crystals, J. Cryst. Growth, 285, 215–227, doi:10.1016/j.jcrysgro.2005.08.007, 2005.
Shultz, M. J., Bisson, P. J., and Brumberg, A.: Best face forward: crystal-face competition at the ice–water interface, J. Phys. Chem. B, 118, 7972–7980, doi:10.1021/jp500956w, 2014.
Smith, R.: Conquering chemistry, 4th ed., McGraw-Hill, Sydney, XIV, 344 pp., 2004.
Thomas, A. C.: Growth of thin Film Water on α-Al_2O_3 (0001) and its Implications for Ice Nucleation, Ohio University, Ohio, USA, 2009.
Yang, Z., Bertram, A. K., and Chou, K. C.: Why do sulfuric acid coatings influence the ice nucleation properties of mineral dust particles in the atmosphere?, J. Phys. Chem. Lett., 2, 1232–1236, doi:10.1021/jz2003342, 2011.
Zhang, W.-K., Zheng, D.-S., Xu, Y.-Y., Bian, H.-T., Guo, Y., and Wang, H.-F.: Reconsideration of second-harmonic generation from isotropic liquid interface: broken Kleinman symmetry of

AMTD
8, 5265–5282, 2015

neat air/water interface from dipolar contribution, J. Chem. Phys., 123, 224713-1–224713-11, doi:10.1063/1.2136875, 2005.
Zhang, Y., Macke, A., and Albers, F.: Effect of crystal size spectrum and crystal shape on stratiform cirrus radiative forcing, Atmos. Res., 52, 59–75, doi:10.1016/S0169-8095(99)00026-5, 1999.
Zhang, Y., Anim-Danso, E., and Dhinojwala, A.: The effect of a solid surface on the segregation and melting of salt hydrates, J. Am. Chem. Soc., 136, 14811–14820, doi:10.1021/ja5067866, 2014.
Zhuang, X., Miranda, P. B., Kim, D., and Shen, Y. R.: Mapping molecular orientation and conformation at interfaces by surface nonlinear optics, Phys. Rev. B, 59, 12632–12640, 1999.

AMTD
8, 5265–5282, 2015

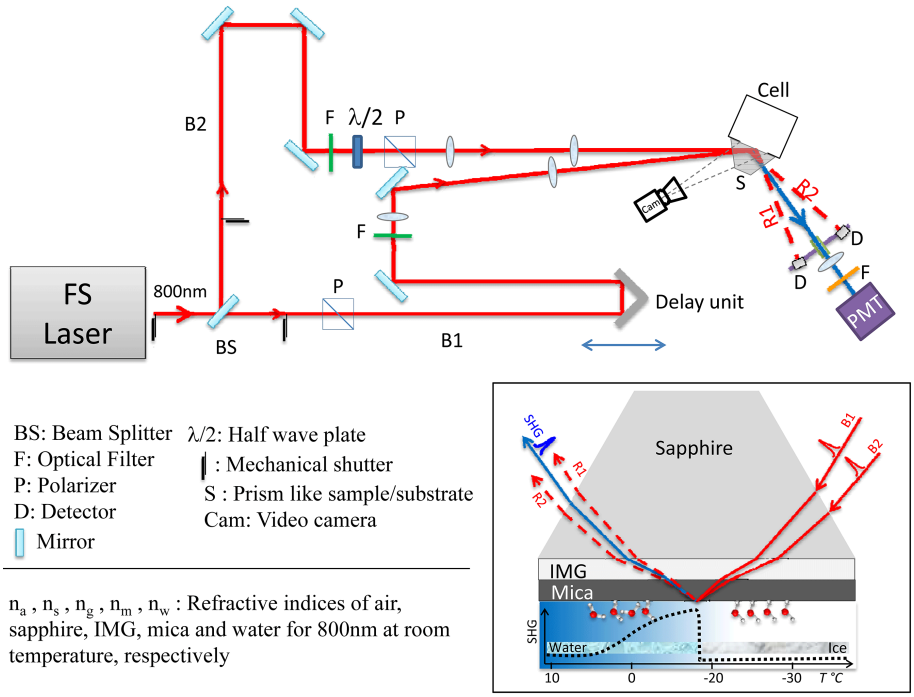

Figure 1. A schematic presentation of the SHG setup used in this study. Inset shows the sample geometry. See text for detailed explanations.

AMTD
8, 5265–5282, 2015

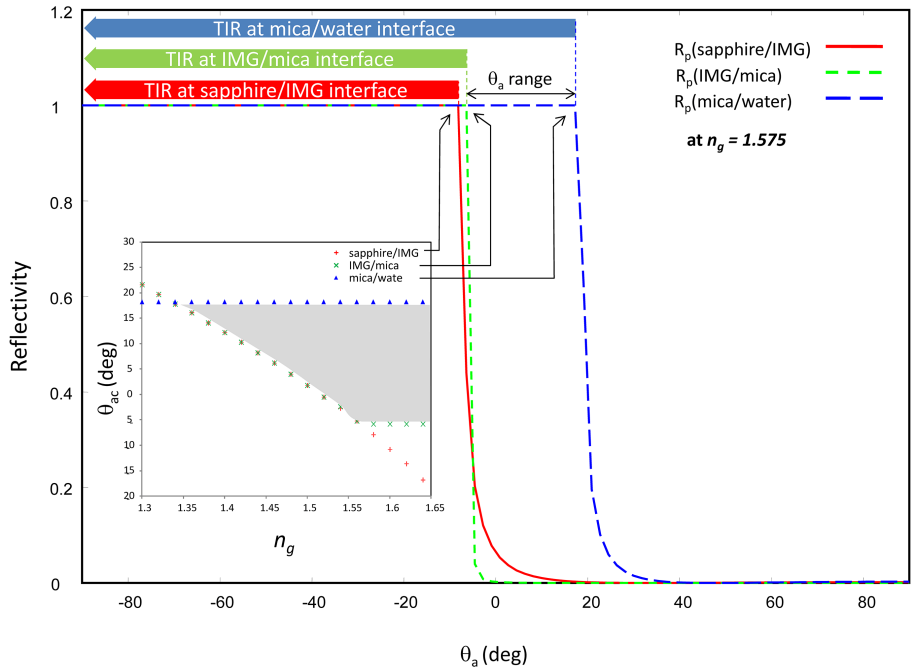

Figure 2. Reflectivities of a P-polarized (Rp) light as a function of the incident angle from air (θ_a) at the different interfaces of inset Fig. 1. The reflectivities at sapphire/IMG, IMG/mica and mica/water interfaces are represented by the soli-red, dash-green and long-dash-blue lines respectively. An arbitrary value of n_g = 1.575 is chosen. The points of drop of the reflectivity for the three interfaces as a function of n_g are plotted on the inset. θ_{ac} is the lower threshold of θ_a for the sapphire/IMG and IMG/mica interfaces and the higher threshold of θ_a for mica/water interface. The shaded area is the range of allowed incident angles from air at any n_g.

AMTD
8, 5265–5282, 2015

Probing ice-nucleation processes on the molecular level

A. Abdelmonem et al.

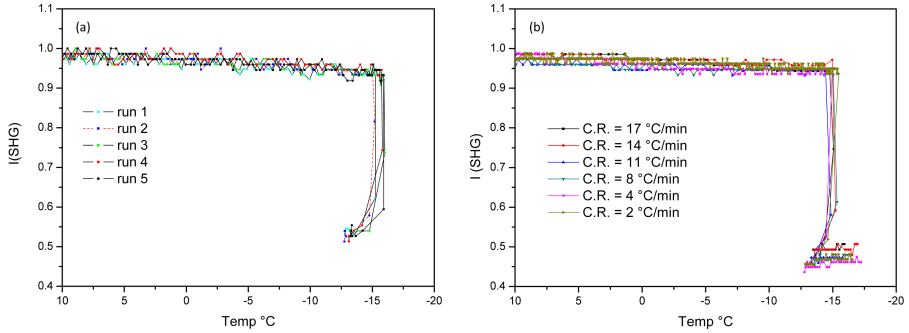

Figure 3. SHG at sapphire/water-ice interface as a function of temperature during cooling. **(a)** The same cooling profile of $-8\,^{\circ}\mathrm{C\,min^{-1}}$ cooling rate is repeated 5 times. **(b)** Different cooling rates.

AMTD
8, 5265–5282, 2015

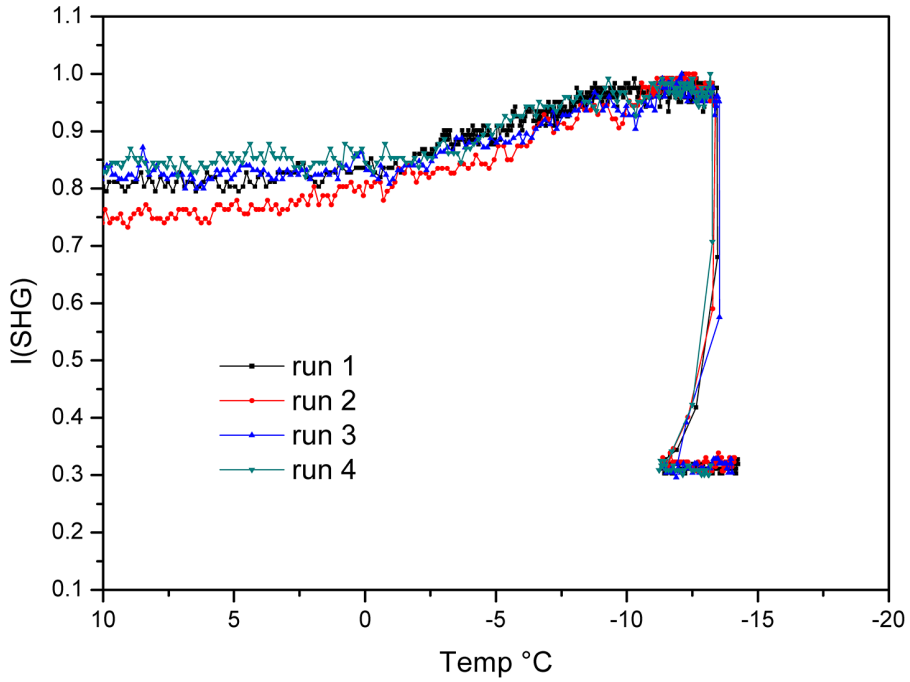

Figure 4. SHG at mica/water-ice interface as a function of temperature during cooling at a cooling rate of −2 °C min.

AMTD
8, 5265–5282, 2015